European Journal of Radiology 190 (2025) 112246

Contents lists available at ScienceDirect

European Journal of Radiology

journal homepage: www.elsevier.com/locate/ejrad

Dynamic contrast-enhanced CT-derived extracellular volume fraction for predicting postoperative oncologic outcomes in pancreatic ductal adenocarcinoma

Hideyuki Fukui [a,*], Yasunari Fukuda [b,d], Hiromitsu Onishi [a], Takashi Ota [a], Atsushi Nakamoto [a], Toru Honda [a], Ryo Aihara [a], Yukihiro Enchi [c], Daisaku Yamada [b], Shogo Kobayashi [b], Hidetoshi Eguchi [b], Mitsuaki Tatsumi [a], Noriyuki Tomiyama [a]

[a] Department of Diagnostic and Interventional Radiology, Osaka University Graduate School of Medicine, Japan
[b] Department of Gastroenterological Surgery, Osaka University Graduate School of Medicine, Japan
[c] Division of Radiology, Department of Medical Technology, Osaka University Hospital, Japan
[d] Department of Gastroenterological Surgery, Kindai University Nara Hospital, Japan

ARTICLE INFO

Keywords:
Pancreatic ductal adenocarcinoma
Computed tomography: X-ray
Extracellular space
Prognosis
Survival analysis

ABSTRACT

Objective: To evaluate the prognostic value of the extracellular volume fraction (fECV) derived from contrast-enhanced computed tomography (CE-CT) for recurrence-free survival (RFS) and overall survival (OS) rates after pancreatic ductal adenocarcinoma (PDAC) surgery.

Methods: This retrospective study evaluated 71 patients diagnosed with PDAC postsurgery who underwent CE-CT with precontrast and equilibrium phases before neoadjuvant chemotherapy (35 males, 36 females; mean age, 70.3 years; 95 % CI, 68.1–72.6; SD, 9.8; range, 45–89 years), were enrolled. Noncancerous pancreatic parenchyma and pancreatic tumors were automatically segmented from nonenhanced and equilibrium-phase images, excluding focal lesions, major-vessel, and ducts. Uni- and multivariate analyses (Cox proportional hazards model) were performed to evaluate fECV [=(100 − hematocrit) × (ΔPancreas/ΔAorta] in the nonaffected pancreas and tumor, with age, sex, chemotherapeutic scheme, tumor marker/location/size, stage, histological type, RFS, and OS as factors. Time-dependent receiver-operating characteristic curves showed the optimal fECV cutoff values for predicting RFS and OS.

Results: Adjuvant chemotherapy regimen, histological type, and fECV of noncancerous pancreatic parenchyma were independent prognostic factors of OS ($p < 0.001$, 0.049, and 0.018, respectively), and TNM stage (IB) was an independent predictor of RFS ($p = 0.025$). RFS and OS were worse in patients with noncancerous pancreatic tissue with higher fECV than in those with lower fECV (optimal cutoffs: 40.32 % for RFS, $p = 0.036$; 43.65 % for OS, $p < 0.001$).

Conclusion: The fECV of noncancerous pancreatic parenchyma from CE-CT was a significant predictor of survival outcomes in PDAC.

1. Introduction

Pancreatic ductal adenocarcinoma (PDAC) is an oncological disease with high mortality and poor prognosis, although there have been advances in diagnostic imaging and therapeutic strategies [1,2]. Accurate prognostication of postoperative outcomes is crucial for optimizing patient care and treatment planning [3–9]. Currently, prognostic prediction in PDAC heavily relies on clinicopathological parameters, such as tumor stage, grade, and markers [1,2,10]. However, these factors alone may not fully capture the heterogeneity of PDAC and the complex tumor–microenvironment interplay [8,11].

In recent years, quantitative imaging features derived from contrast-enhanced computed tomography (CE-CT) have shown promise in predicting survival outcomes in PDAC [3–9,11–18]. Specifically, the

* Corresponding author at: Department of Diagnostic and Interventional Radiology, Osaka University Graduate School of Medicine, D1, 2-2, Yamadaoka, Suita, Osaka 565-0871, Japan.
E-mail address: hidefukui@infoseek.jp (H. Fukui).

https://doi.org/10.1016/j.ejrad.2025.112246
Received 3 April 2025; Received in revised form 2 June 2025; Accepted 16 June 2025
Available online 18 June 2025

extracellular volume fraction (fECV), calculated from dynamic CE-CT, has emerged as an imaging parameter potentially useful for predicting PDAC [14–17,19]. The fECV reflects the extracellular space, which is influenced by factors, such as vascularity, cellularity, and fibrosis [11,20–22]. Previous studies have demonstrated associations between fECV and overall survival (OS) in patients undergoing chemotherapy for unresectable stage IV PDAC [14,15,19]. Most studies have predominantly focused on unresectable or metastatic pancreatic cancer. Nevertheless, the fECV value for predicting recurrence-free survival (RFS) and OS rates in postsurgical settings remains unclear. Additionally, optimal cutoff values for fECV in predicting survival outcomes for patients who underwent surgical resection have not been determined. Furthermore, the relative prognostic significance of fECV in the context of other clinicopathological factors in resected PDAC patients warrants further investigation.

Recent evidence suggests that the tumor microenvironment in PDAC extends beyond the tumor itself, particularly reaching the surrounding pancreatic parenchyma. This has potential implications for disease progression and patient outcomes. Pancreatic fibrosis is characterized by excessive deposition of extracellular matrix mediated by activated pancreatic stellate cells. This condition creates a microenvironment that may influence cancer growth and invasion, as well as the therapeutic response [23–26]. Chen et al. showed that fibrosis in the residual pancreas after surgery was associated with poor prognosis in patients with PDAC [27]. These finding indicate that the condition of noncancerous pancreatic tissues can provide valuable prognostic information. fECV reflects extracellular space, which is influenced by factors such as fibrosis, vascularity, and cellularity [11,20–22]. Thus, we hypothesized that fECV measurements in noncancerous pancreatic parenchyma may capture important prognostic information not reflected by tumor-centric parameters alone. Previous studies have primarily focused on tumor-derived imaging biomarkers of PDAC [3,5–9,11–18,28]. However, the potential prognostic significance of quantitative imaging parameters in the noncancerous pancreatic parenchyma remains unexplored.

Therefore, the study aim of this retrospective study was to assess the value of the fECV derived from CE-CT for predicting RFS and OS after PDAC surgery. We investigated the associations between survival outcomes and the factors of noncancerous pancreatic parenchyma and tumor fECV values and then determined the optimal cutoff values for fECV for evaluating RFS and OS. By assessing the prognostic significance of fECV in the context of other clinicopathological factors, we hope to provide insights into the potential utility of fECV as an imaging parameter for risk stratification and prognostication in postoperative patients with PDAC.

2. Materials and methods

This study was approved by the Institutional Review Board at Osaka University Hospital (Approval Number: [20351]), and informed consent was waived in accordance with ethical regulations for retrospective studies, adhering to human rights declarations.

2.1. Patients

This retrospective study analyzed data from patients examined between January 2014 and February 2022. We evaluated 541 consecutive patients, who underwent pancreatectomy between January 2014 and February 2022 at our institution. Patients meeting the following criteria were included in the analysis: (1) pathologically described as pancreatic ductal adenocarcinoma, (2) had undergone preoperative CE-CT, including unenhanced and equilibrium phases, and (3) had not received preoperative therapy before CT. Among the 541 consecutive patients who underwent pancreatectomy, 235 were diagnosed with PDAC (criterion 1). Of them, 101 had available unenhanced and equilibrium phase CT scan images (criterion 2), and 90 did not receive preoperative therapy before CT scan (criterion 3). Among the remaining 90 patients, 7 having severe pancreatic atrophy and ductal dilatation that prevented reliable fECV measurements due to insufficient viable pancreatic parenchyma and 9 with signs of acute pancreatitis on diagnostic CT imaging or laboratory tests were not included [29]. Three patients with missing survival information were also excluded. Eventually, 71 consecutive patients (35 males and 36 females; mean ± SD age, 70.3 ± 9.8 years; 95 % CI, 68.1–72.6; age range, 45–89 years) were enrolled (Fig. 1). Among them, 34 and 37 underwent pancreaticoduodenectomy and distal pancreatectomy, respectively. The median interval between the procedure and CT imaging was 93 days (interquartile range [IQR, 69–115] range, 5–281).

2.2. CT imaging

CT imaging was performed on a 320-channel (Aquilion One Genesis Edition; Canon Medical Systems, Otawara, Japan), 160-channel (Aquilion Precision; Canon Medical Systems), or 64-channel (Discovery CT 750 HD or Discovery CT 750 HD Freedom Edition; GE Healthcare) instrument. The following scanning conditions were used: collimation: 0.625 × 64 or 0.5 × 80 mm^2; pitch: 1.375 or 0.813 mm/rotation; rotation time: 0.4 or 0.5 s/rotation; exposure parameters: 120 kV with autoexposure monitoring, a noise index standard deviation of 13.8 or 15, and a field of view of 345 mm. Image conversion was performed with a slice thickness of 5 mm and either an FC03 or GE standard kernel. We used the CTDIvol to evaluate patient radiation exposure, and the median value was 8.66 mGy. Early arterial phases were received 8 s after achieving 100-HU attenuation of the descending aorta (bolus-tracking method) after obtaining a precontrast scan. Late arterial phases were processed 7 s after the early phase or 20 s after achieving 100-HU attenuation of the descending aorta (with the bolus-tracking method). The portal and equilibrium phases were received 30 s after the late arterial phase and 120 s after the portal phase. Contrast iodine of 600 mg I/kg body weight was administered intravenously at 30 s. Unenhanced and dynamic contrast-enhanced images were acquired, but only the former and equilibrium-phase images were processed. A nonlinear nonrigid registration protocol (SURE SUBTRACTION Iodine Mapping, Canon Medical Systems, Tokyo, Japan: SSIM) was used to produce subtraction images [30].

2.3. Quantitative image evaluation

The fECV evaluations were conducted on an image workstation (SYNAPSE VINCENT; FUJIFILM Medical Co., Ltd., Tokyo, Japan), which uses FUJIFILM's deep learning-based medical AI technology "REiLI." This system was specifically developed to overcome the challenges of pancreatic segmentation through a combination of traditional machine learning methods and specialized deep learning algorithms. The noncancerous pancreatic parenchyma and pancreatic tumors were automatically segmented on these subtraction images derived from nonenhanced and equilibrium-phase images by a workstation application. To ensure an accurate delineation of relevant structures, all automated segmentations were reviewed and, if necessary, manually corrected by a board-certified radiologist (H.F.) with 14 years of experience in abdominal radiology. The segmentation process separately identified and delineated the noncancerous pancreatic parenchyma and the pancreatic tumors. The segmentation excluded focal lesions, major vessels, and ducts. To measure the noncancerous pancreatic parenchyma, only the contralateral portion of the tumor, separated by an estimated transection line, was included in the analysis to prevent any potential influence from peritumoral changes. For ambiguous regions, the correlation with other imaging phases was used to facilitate an accurate differentiation. Tumor fECV and noncancerous pancreatic parenchyma fECV were calculated independently using their respective segmentations. Pancreatic fatty infiltration could affect the fECV; thus, a low threshold was set to eliminate it to the maximum extent, with the preservation of pancreatic parenchymal tissue to decrease the potential

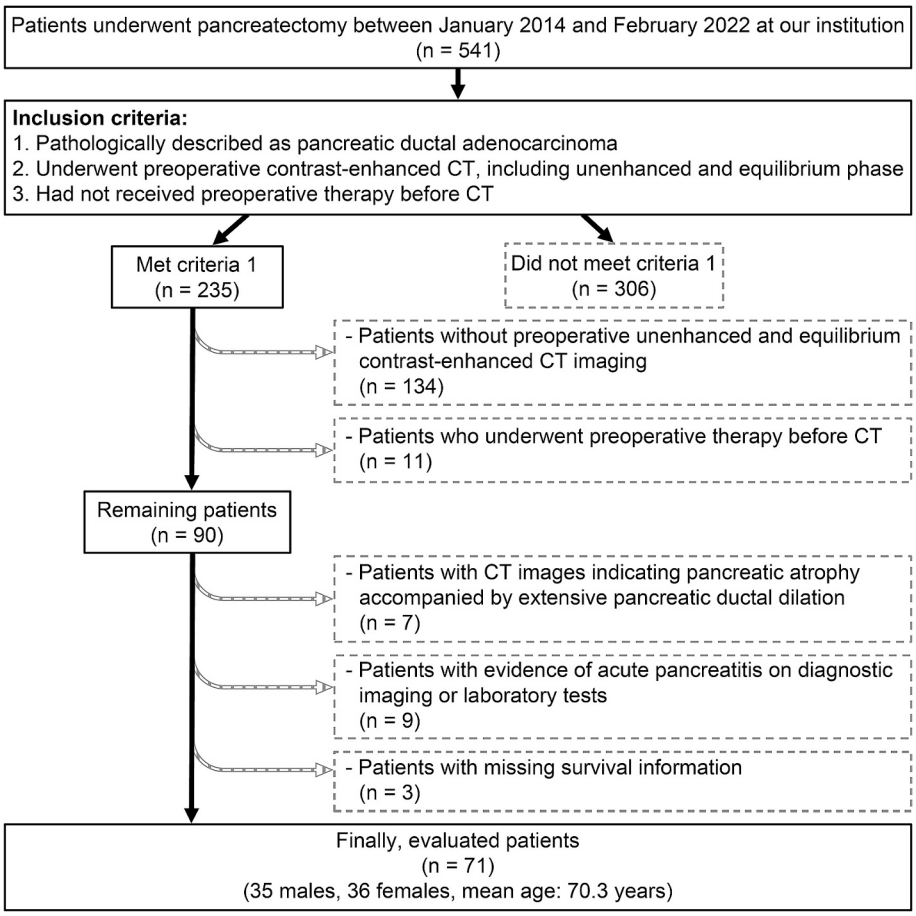

Fig. 1. Flowchart of patient inclusion.

influence of fatty infiltration on fECV evaluations [31]. The mean enhancement degree (in HU) of the noncancerous pancreatic parenchyma and pancreatic tumors (ΔPancreas and ΔTumor) were determined. Regions of interest were outlined as large as possible in the lumen of the aorta and portal vein, not including the vessel wall, to assess the enhancement degree of the aorta (ΔAorta) and portal vein (ΔPortal). ΔAorta and ΔPortal (more than ±10 HU) with significant differences were regarded as outliers and were not included [32]. The noncancerous pancreatic parenchyma and pancreatic tumors fECV were determined with the following equation: fECV [%] = (100 − hematocrit [%]) * ΔPancreas (or ΔTumor)/ΔAorta [30,33] (Fig. 2). The hematocrit levels nearest to the CT exam date were used for analysis. On average, these measurements were taken 2.87 days from the CT exam (95 % CI: 1.74–4.0 days; SD: 4.81 days; range: −14 to 17 days).

2.4. Statistical analysis

The Shapiro–Wilk test was performed to test for normality of the data distribution. Univariate and multivariate analyses using the Cox proportional hazards model were performed to investigate the influence of various factors (including age; sex; neoadjuvant and adjuvant therapeutic regimens; serum CEA, CA19-9, and Duke-pancreatic-monoclonal-antigen type 2 (DUPAN-2) levels; and tumor characteristics, such as location, size, TNM stage, histological type, and tumor and noncancerous pancreatic parenchyma; fECV) on RFS and OS rates. [14,15]. For factors with three or more levels, the Wald test was performed to calculate the *p* value for the entire factor. To determine the optimal cutoff values for the tumor fECV and noncancerous pancreatic parenchyma fECV in predicting RFS and OS, time-dependent receiver-

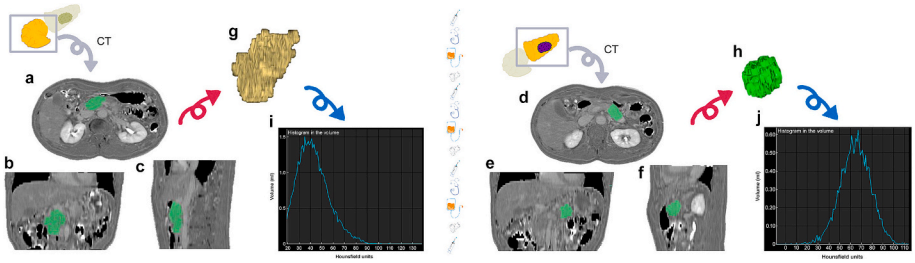

Fig. 2. Images from a 64-year-old male patient with PDAC who underwent distal pancreatectomy: The green areas on the subtraction preoperative CT images, taken between the unenhanced and equilibrium phases, indicate the segmentation of the pancreatic parenchyma in noncancerous areas on the side opposite to the PDAC extending from the estimated transection line **(a–c)** as well as the PDAC itself **(d–f)**. The three-dimensional volumes are shown **(g, h)**. CT histogram showing the CT value of the green area and its distribution percentage **(i, j)**. PDAC: Pancreatic ductal adenocarcinoma, CT: Computed tomography. (For interpretation of the references to colour in this figure legend, the reader is referred to the web version of this article.)

operating characteristic (ROC) curves were constructed, and the cutoff values were determined by maximizing the Youden index. To evaluate the additive value of fECV in predicting OS, we constructed two prediction models. The first model included significant traditional markers, whereas the second model additionally incorporated noncancerous pancreatic parenchymal fECV. Risk scores for each patient were determined using the coefficients from the Cox proportional hazard models. We then performed time-dependent ROC analysis to compare the predictive performance of these models. Furthermore, the comparison of AUCs between models was conducted using the compare C package in R software. The Kaplan–Meier analysis with the log-rank test were performed to compare the RFS and OS between patients with fECV values above and below the optimal ROC-derived cutoff points for tumor and noncancerous pancreatic parenchyma. EZR version 1.50 software (Saitama Medical Center, Jichi Medical University) was used to analyze the data statistically, and values of $p < 0.05$ were accepted as indicating statistical significance.

3. Results

This study evaluated 71 patients (35 men and 36 women; mean age: 70.3 ± 9.8 [range: 45–89] years) with pathologically confirmed PDAC who underwent surgical resection. Table 1 shows the characteristics of the patients.

We conducted univariate and multivariate Cox hazard analyses to evaluate the predictive role of various factors, including the fractional extracellular volume (fECV) of the tumor and pancreatic parenchyma in noncancerous areas, for assessing OS and RFS rates in patients with pancreatic cancer. Of the 71 patients, 43 (60.6 %) died, and 47 (66.2 %) exhibited recurrence during the follow-up period. In our patient cohort, the median OS was 26 (range: 9.1–89.7) months, with RFS having a median of 16 (range: 1.8–89.7) months. Time-dependent ROC curve analyses were performed to determine the optimal cutoff values of noncancerous pancreatic parenchymal fECV and tumor fECV for predicting OS and RFS. For noncancerous pancreatic parenchymal fECV, the areas under the ROC curve (AUCs) were 0.687 for OS and 0.672 for RFS. The optimal cutoff values were 43.65 % for OS (sensitivity: 0.677, specificity: 0.758) and 40.32 % for RFS (sensitivity: 0.818, specificity: 0.571). For tumor fECV, the AUCs were 0.598 for OS and 0.590 for RFS, with optimal cutoff values of 47.45 % (sensitivity: 0.531, specificity: 0.711) and 38.00 % (sensitivity: 0.864, specificity: 0.367), respectively. The noncancerous pancreatic parenchymal fECV (>43.65 %) was found to be a significant independent prognostic factor of OS in multivariate (hazard ratio: 2.52, 95 % CI: 1.17–5.44, $p = 0.018$) analyses. Higher fECV values in the noncancerous pancreatic parenchyma were indicative of higher risks of mortality. However, tumor fECV was not an efficient predictor of either OS or RFS rates in our study. Adjuvant therapy was identified as a significant predictor of OS in multivariate ($p < 0.001$) analyses. Patients who received gemcitabine as adjuvant therapy had a significantly higher mortality risk than those not subjected to any adjuvant therapy (hazard ratio: 11.87, 95 % CI: 3.18–44.25, $p < 0.001$). However, there were no significant differences in the risk of mortality between the patients who underwent S-1 as adjuvant therapy and those who did not receive any adjuvant therapy (hazard ratio: 1.45, 95 % CI: 0.67–3.14, $p = 0.346$). The histological type was indicative of a higher risk for mortality ($p = 0.049$). In the multivariate analysis, the risk of recurrence was only significantly higher for TNM stage IB disease than for stage IA disease (hazard ratio: 2.31, 95 % CI: 1.11–4.81, $p = 0.025$). The risk of recurrence was not significantly different for Stages II and III than for stage IA in the multivariate analysis. Other parameters, including age, sex, neoadjuvant therapy, tumor location, and serum levels of CEA, CA 19–9, and DUPAN-2, did not show significant associations with OS or RFS in the and multivariate analyses (Tables 2 and 3).

To further evaluate the contribution of fECV measurements to survival prediction, further time-dependent ROC analyses comparing multiple predictive models were performed. For OS prediction, the following three models were compared: model 1, which incorporated traditional OS predictors only (histological type and adjuvant therapy; AUC = 67.71 %); model 2, which additionally included noncancerous pancreatic parenchymal fECV (AUC = 81.33 %); and model 3, which comprised both noncancerous pancreatic parenchymal fECV and tumor fECV (AUC = 84.61 %). Based on a statistical comparison, a significant improvement was observed in model 2 versus model 1 (p = 0.040) and model 3 versus model 1 (p = 0.036). However, model 3 and model 2 did not significantly differ (p = 0.455).

Similarly, for RFS prediction, the following were compared: model 1 with TNM stage only (AUC = 55.93 %); model 2 with TNM stage and noncancerous pancreatic parenchymal fECV (AUC = 68.42 %); and model 3 with TNM stage and noncancerous pancreatic parenchymal fECV and tumor fECV (AUC = 69.19 %). Both model 2 and model 3 exhibited significant improvement compared with model 1 (p < 0.001 for both). Meanwhile, model 3 and model 2 did not significantly differ (p = 0.655).

In the Kaplan–Meier analysis with log-rank tests (Fig. 3), patients with fECV values of the pancreatic parenchyma in noncancerous areas above the optimal ROC-derived cutoff (43.65 % for OS and 40.32 % for RFS) had significantly lower median OS and RFS times than those of patients with fECV values below the cutoffs (OS: 19.2 vs. 39.7 months, $p < 0.001$; RFS: 8.8 vs. 21.5 months, $p = 0.036$). In contrast, tumor fECV values above and below the optimal ROC-derived cutoffs (47.45 % for OS and 38.00 % for RFS) did not show statistically significant differences in either OS ($p = 0.1$) or RFS ($p = 0.8$) between the two groups.

Patients with tumors in the pancreatic head exhibited significantly higher fECV values in noncancerous pancreatic parenchyma than those with tumors in the pancreatic body/tail (median: 44.32 % vs. 40.01 %, p

Table 1
Baseline characteristics of the patients with pancreatic ductal adenocarcinoma.

Characteristics of the patients	Value*
Age (years)	70.3 ± 9.8 (45–89)
Sex	
Male	35 (49.3 %)
Female	36 (50.7 %)
Tumor location	
Head	30 (42.3 %)
Body	24 (33.8 %)
Tail	17 (23.9 %)
TNM stage	
IA	25 (35.2 %)
IB	38 (53.5 %)
II	2 (2.8 %)
III	6 (8.5 %)
Histological type	
Well-differentiated adenocarcinoma	35 (49.3 %)
Moderately differentiated adenocarcinoma	29 (40.8 %)
Poorly differentiated adenocarcinoma	7 (9.9 %)
Surgical procedure	
Pancreaticoduodenectomy	34 (47.9 %)
Distal pancreatectomy	37 (52.1 %)
Neoadjuvant therapy	
None	18 (25.4 %)
GS	20 (28.2 %)
GN	17 (23.9 %)
GS-RT	11 (15.5 %)
GN-RT	3 (4.2 %)
GEM-RT	2 (2.8 %)
Adjuvant therapy	
None	16 (22.5 %)
S-1	50 (70.4 %)
GEM	5 (7.0 %)

*Values were presented as the mean ± standard deviation (range) or the number (percentage) as appropriate.
Abbreviations: TNM, tumor–node–metastasis; GS, gemcitabine and S-1 combination therapy; GN, gemcitabine and nab-paclitaxel combination therapy; RT, radiation therapy; GEM, gemcitabine.

Table 2
Uni- and multivariate Cox hazard analyses for RFS in patients with pancreatic cancer.

Variable	Patients	Univariate analysis			Multivariate analysis		
		Hazard ratio	95 % confidence intervals	*p* value	Hazard ratio	95 % confidence intervals	*p* value
Age (years)		0.98	0.95–1.01	0.282			
Sex				0.825			
Female	36	1					
Male	35	1.06	0.60–1.87				
Neoadjuvant therapy				0.266			
None	18	1					
GS	20	0.43	0.19–0.99	0.048			
GN	17	0.53	0.24–1.15	0.109			
GS-RT	11	0.81	0.34–1.92	0.633			
GN-RT	3	0.75	0.17–3.29	0.701			
GEM-RT	2	1.71	0.38–7.62	0.482			
Adjuvant therapy				0.068			0.233
None	16	1					
S-1	50	0.99	0.47–2.09	0.954	1.1	0.53–2.29	0.797
GEM	5	3.1	1.02–9.46	0.047	2.65	0.80–8.78	0.111
CEA (ng/mL)		1.01	0.96–1.06	0.77			
CA 19–9 (U/mL)		1	1.00–1.00	0.729			
DUPAN-2 (U/mL)		1	1.00–1.00	0.209			
Tumor location				0.604			
Head	30	1					
Body	24	0.71	0.36–1.39	0.316			
Tail	17	0.89	0.43–1.84	0.752			
TNM stage				0.06			0.162
IA	25	1					
IB	38	2.6	1.15–4.96	0.007	2.31	1.11–4.81	0.025
II	2	2.83	0.11–7.00	0.18	2.80	0.49–16.03	0.248
III	6	1.9	0.65–5.45	0.24	1.82	0.61–5.46	0.283
Histological type				0.24			
Well-differentiated adenocarcinoma	35	1					
Moderately differentiated adenocarcinoma	29	1.61	0.88–2.96	0.123			
Poorly differentiated adenocarcinoma	7	1.73	0.65–4.59	0.27			
Tumor size		0.99	0.94–1.04	0.65			
Tumor fECV (>38.00 %)	50	1.08	0.58–2.02	0.841	1.191	0.59–2.39	0.624
fECV of pancreatic parenchyma in noncancerous areas (>40.32 %)	39	1.86	1.03–3.34	0.039	1.72	0.91–3.27	0.097

RFS: Recurrence-free survival, GS: Gemcitabine and S-1 combination therapy, GN: Gemcitabine and nab-paclitaxel combination therapy, RT: Radiation therapy, GEM: Gemcitabine, CEA: Carcinoembryonic antigen, CA19-9: Carbohydrate antigen 19–9, DUPAN-2: Duke-pancreatic-monoclonal-antigen type 2, TNM: Tumor–node–metastasis, fECV: Fractional extracellular volume.
*Data in parentheses are the medians and ranges.

= 0.014) (Fig. 4). In patients with pancreatic head tumors (n = 30), those with high fECV (≥43.65 %) showed significantly worse OS than patients with low fECV (median survival: 19.2 vs. 38.7 months, $p < 0.001$). Similarly, in patients with pancreatic body/tail tumors (n = 41), high fECV was associated with significantly worse OS (median survival: 17.4 vs. 29.2 months, p = 0.028) (Fig. 5A, 5B). For pancreatic head tumors, the difference in the RFS between patients with a high noncancerous pancreatic parenchymal fECV (≥40.32 %) and a low fECV did not reach statistical significance (median RFS: 7.6 vs 15.1 months, p = 0.324). Similarly, for pancreatic body/tail tumors, a significant difference was not observed in terms of RFS between the high and low fECV groups (median RFS: 5.2 vs 13.9 months, p = 0.089) (Fig. 5C, 5D).

4. Discussion

In this study, we assessed the predictive value of fECV in tumor and pancreatic parenchyma in noncancerous areas for OS and RFS in patients with PDAC. Our results showed that the fECV of the pancreatic parenchyma in noncancerous areas was a significant independent predictor of OS; however, tumor fECV was not significantly associated with either OS or RFS.

The univariate and multivariate Cox hazard analyses showed that higher fECV values in noncancerous pancreatic parenchyma were associated with a higher risk of mortality. This finding suggests that the microenvironment of the noncancerous pancreatic parenchyma has a role in the progression and prognosis of PDAC. Our findings are in accordance with those of Chen et al., which showed that fibrosis in the residual pancreas was correlated with poor prognosis [27]. The biological basis for this correlation can be explained via several key mechanisms: First, activated pancreatic stellate cells in the fibrotic parenchyma produce extracellular matrix proteins and growth factors that create a microenvironment favorable for cancer progression. Second, parenchymal fibrosis impairs drug delivery by increasing interstitial fluid pressure and reducing functional vasculature, thereby compromising treatment efficacy. Third, inflammation in noncancerous tissues leads to the production of pro-inflammatory cytokines that promote cancer cell survival, invasion, and metastatic potential [23,24]. These pathophysiological processes can extend their influence beyond the primary tumor site, which affects the whole pancreatic tissue and, ultimately, patient outcomes. The high fECV values observed likely reflected a more extensive fibrosis in the pancreatic microenvironment. Thus, fECV can be a noninvasive imaging biomarker for quantifying this clinically relevant feature. Fibrosis tends to be a primary contributor to elevated fECV. However, fECV may also reflect other biological processes including altered vascularity, inflammatory changes, and modified interstitial fluid dynamics in the pancreatic microenvironment [23,24]. These combined mechanisms could enhance tumor progression via impaired drug delivery, hypoxia, pro-inflammatory signaling, and altered mechanical forces, potentially explaining the observed correlation between higher fECV values and poor prognosis.

A novel aspect of our study is that it specifically investigated the prognostic value of fECV after surgery for PDAC patients, particularly

Table 3
Uni- and multivariate Cox hazard analyses for OS in patients with pancreatic cancer.

Variable	Patients	Univariate analysis			Multivariate analysis		
		Hazard ratio	95 % confidence intervals	*p* value	Hazard ratio	95 % confidence intervals	*p* value
Age (years)		0.99	0.95–1.02	0.348			
Sex				0.825			
Female	36	1					
Male	35	1.07	0.59–1.95				
Neoadjuvant therapy				0.248			
None	18	1					
GS	20	0.75	0.32–1.76	0.515			
GN	17	0.51	0.21–1.21	0.125			
GS-RT	11	0.94	0.40–2.26	0.898			
GN-RT	3	1.77	0.40–7.93	0.454			
GEM-RT	2	2.98	0.66–13.55	0.157			
Adjuvant therapy				0.032			<0.001
None	16	1					
S-1	50	0.99	0.47–2.09	0.974	1.45	0.67–3.14	0.346
GEM	5	3.53	1.16–10.70	0.026	11.87	3.18–44.25	<0.001
CEA (ng/mL)		0.98	0.92–1.04	0.495			
CA 19–9 (U/mL)		1	1.00–1.00	0.765			
DUPAN-2 (U/mL)		1	1.00–1.00	0.302			
Tumor location				0.671			
Head	30	1					
Body	24	0.79	0.39–1.61	0.522			
Tail	17	0.73	0.34–1.56	0.421			
TNM stage				0.112			0.328
IA	25	1					
IB	38	2.39	1.15–4.96	0.020	1.88	0.79–4.48	0.155
II	2	0.89	0.11–7.00	0.913	0.46	0.05–4.64	0.510
III	6	1.91	0.60–6.16	0.277	1.79	0.50–6.41	0.370
Histological type				0.075			0.049
Well-differentiated adenocarcinoma	35	1					
Moderately differentiated adenocarcinoma	29	2.02	1.06–3.86	0.032	2.14	1.06–4.32	0.034
Poorly differentiated adenocarcinoma	7	2.12	0.77–5.80	0.143	2.77	0.96–7.97	0.059
Tumor size		0.99	0.92–1.05	0.675			
Tumor fECV (>47.45 %)	26	1.61	0.85–3.05	0.147	2.11	0.95–4.67	0.066
fECV of Pancreatic parenchyma in noncancerous areas (>43.65 %)	27	3.21	1.71–6.02	<0.001	2.52	1.17–5.44	0.018

OS: Overall survival, GS: Gemcitabine and S-1 combination therapy, GN: Gemcitabine and nab-paclitaxel combination therapy, RT: Radiation therapy, GEM: Gemcitabine, CEA: Carcinoembryonic antigen, CA19-9: Carbohydrate antigen 19–9, DUPAN-2: Duke-pancreatic-monoclonal-antigen type 2, TNM: Tumor–node–metastasis, fetch: Fractional extracellular volume.
*Data in parentheses are the medians and ranges.

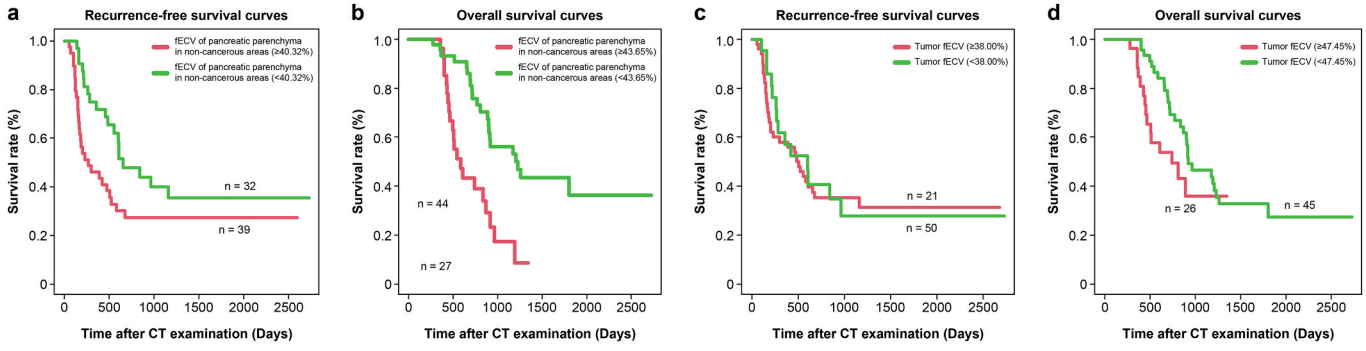

Fig. 3. Patients with a higher fECV in pancreatic parenchyma in noncancerous areas had RFS and OS inferior to those of patients with lower fECV levels, as determined from the optimal fECV cutoffs of 40.32 % for RFS and 43.65 % for OS (RFS, $p = 0.036$; OS, $p < 0.001$) **(a, b)**. No statistically significant differences in RFS and OS, determined from the optimal tumor fECV cutoffs of 38.00 % for RFS and 47.45 % for OS, were observed **(c, d)**. fECV: Fractional extracellular volume, RFS: Recurrence-free survival, OS: Overall survival.

focusing on the noncancerous pancreatic parenchyma, which has not been well-studied before. Although previous studies have examined the relationship between various tumor-derived CT parameters and the prognosis of patients with PDAC [3,5–9,11–18,28], we are not aware of any study that has evaluated the prognostic significance of fECV in noncancerous pancreatic parenchyma. Some strengths of our study are the comprehensive assessment of fECV in the tumor and noncancerous pancreatic parenchyma as well as the determination of optimal cutoff values for predicting survival outcomes from time-dependent ROC curve analyses showing cutoff values for fECV with better discriminatory ability for the fECV of the pancreatic parenchyma in noncancerous areas than for the fECV of tumors. For OS and RFS prediction, models incorporating noncancerous pancreatic parenchymal fECV exhibited significant improvement compared with traditional markers alone, with

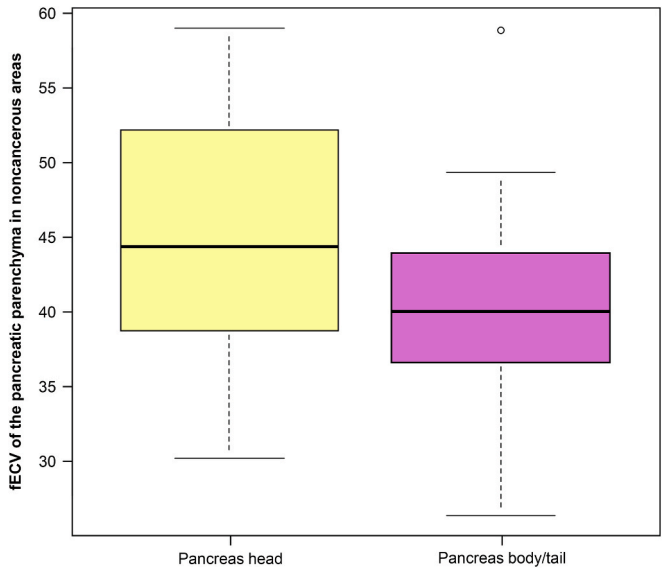

Fig. 4. Comparison of fECV in noncancerous pancreatic parenchyma between tumor locations Box plots showing the distribution of fECV values in noncancerous pancreatic parenchyma for tumors located in the pancreatic head versus body/tail. Patients with tumors in the pancreatic head showed significantly higher fECV values (median: 44.32 %) than those with tumors in the pancreatic body/tail (median: 40.01 %; p = 0.014). fECV: Fractional extracellular volume.

substantial increases in AUC (from 67.71 % to 81.33 % for OS and from 55.93 % to 68.42 % for RFS). Notably, the addition of tumor fECV to models already containing noncancerous pancreatic parenchymal fECV resulted in slight numerical increases in predictive accuracy. However, these increments were not statistically significant, underscoring that the prognostic information is primarily derived from measurements in noncancerous tissues.

Interestingly, tumor fECV was not found to be an important parameter in either OS or RFS in our study. This finding contrasts with those of some former studies [14,15,17,19]. The lack of a significant association between tumor fECV and survival outcomes in our study that focused on resectable PDAC may be due to the relatively small size of the tumors and limited presence of internal necrosis. As demonstrated by Gao et al. [6], larger pancreatic tumors are more prone to necrosis, which can lead to weaker CT enhancement. The tumor relative enhancement ratio was found to be significantly and negatively correlated with tumor size.

The Kaplan–Meier analysis with log-rank tests further confirmed the prognostic significance of the fECV in the pancreatic parenchyma of noncancerous areas. Patients with fECV values greater than the optimal ROC-derived cutoffs had significantly shorter median OS and RFS times than those of patients with fECV values less than the cutoffs. These results highlight the potential utility of the fECV in the pancreatic parenchyma of noncancerous areas as a prognostic marker for risk stratification and personalized treatment strategies in PDAC patients.

Notably, in our study, the association between noncancerous pancreatic parenchymal fECV and OS was stronger than that with RFS. The univariate analysis and log-rank tests showed significant associations between fECV and RFS. However, this correlation eventually had borderline significance (p = 0.097) in the multivariate analysis. This discrepancy can be primarily attributed to statistical factors. The hazard ratio for OS was significantly higher (HR: 2.52–3.21) than that for RFS (HR: 1.72–1.86), thereby indicating a stronger effect size for OS that remained significant across different analytical approaches. In the multivariate analysis of RFS, TNM stage emerged as a stronger predictor (particularly stage IB: HR = 2.31, p = 0.025), potentially diminishing the relative contribution of fECV. These findings suggest that although noncancerous pancreatic parenchymal fECV has prognostic value for both OS and RFS, its independent contribution to RFS prediction is relatively lower compared with that of established clinicopathological factors such as TNM stage.

Our analyses comparing pancreatic head versus body/tail tumors can provide essential insights into the biological basis of the prognostic value of fECV. Notably, patients with pancreatic head tumors had significantly higher noncancerous pancreatic parenchymal fECV than those with body/tail tumors, potentially reflecting the greater mechanical ductal obstruction that typically occurs with head tumors. Interestingly, in the overall cohort, fECV was significantly associated with both OS and RFS. However, when stratified by tumor location (head vs. body/tail), only the association between fECV and OS maintained its statistical significance in both subgroups. Based on this finding, the correlation between fECV and OS is more robust. This may partly reflect reduced statistical power in the subgroup analyses but may also suggest that fibrosis in noncancerous pancreatic tissues has a stronger impact on long-term survival than on immediate tumor recurrence. Nevertheless, the prognostic significance of fECV for OS persisted regardless of tumor location, thereby suggesting that its clinical utility extends across different anatomical presentations of PDAC, particularly for predicting overall survival outcomes. Thus, additional studies with larger sample sizes should be conducted to validate these findings for RFS in location-stratified subgroups.

This study had some limitations. First, our retrospective, single-center study with 71 patients requires validation in larger, multicenter

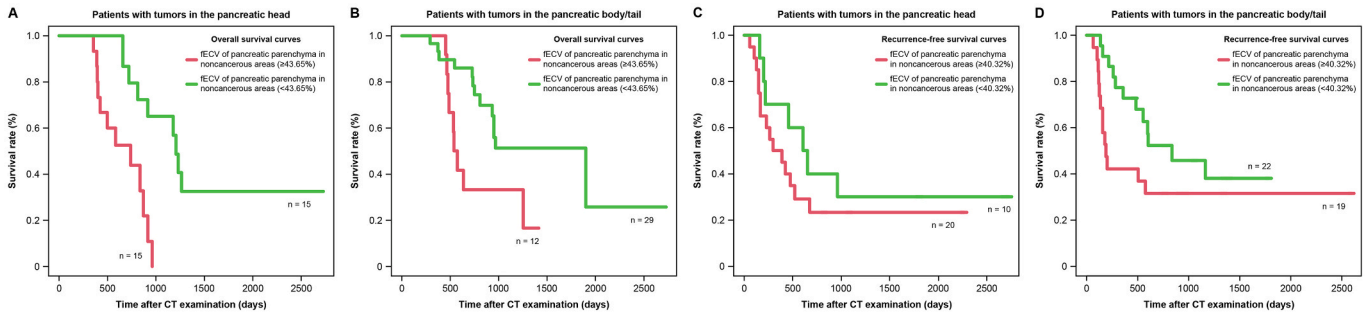

Fig. 5. Kaplan–Meier survival curves stratified by fECV in noncancerous pancreatic parenchyma for different tumor locations. (a) OS in patients with pancreatic head tumors (n = 30). Patients with a high fECV (≥43.65 %) had a significantly worse OS than those with a low fECV (< 43.65 %) (median survival: 19.2 vs. 38.7 months, p < 0.001). (b) OS in patients with pancreatic body/tail tumors (n = 41). Similarly, patients with a high fECV (≥43.65 %) exhibited a significantly worse OS than those with a low fECV (<43.65 %) (median survival: 17.4 vs. 29.2 months, p = 0.028). (c) RFS in patients with pancreatic head tumors (n = 30). The difference in RFS between patients with a high fECV (≥ 40.32 %) and those with a low fECV (<40.32 %) did not reach statistical significance (median RFS: 7.6 vs 15.1 months, p = 0.324). (d) RFS in patients with pancreatic body/tail tumors (n = 41). Similarly, the difference in RFS between patients with a high fECV (≥40.32 %) and those with a low fECV (<40.32 %) did not reach statistical significance (median RFS: 5.2 vs 13.9 months, p = 0.089). fECV: Fractional extracellular volume, *OS*: Overall survival, *RFS*: Recurrence-free survival.

cohorts. Second, a substantial number of patients (134 [57 %] of 235 patients with PDAC) were excluded due to the absence of both unenhanced and equilibrium phase CT scan images. This high exclusion rate could have potentially introduced selection bias. However, the availability of equilibrium phase imaging was primarily determined by the development of our institutional imaging protocols over time rather than by patient-specific clinical factors. Nevertheless, this limitation may affect the generalizability of our findings and emphasize the need to conduct prospective studies with standardized imaging protocols. Third, in some cases, blood sampling was not performed on the day as CT scans were performed. Although recent studies have demonstrated no significant differences between the fECV derived from hematocrit values obtained on the same day of imaging and on different days [34], there still might be a minor difference in the results. Fourth, the 5-mm slice thickness used for the fECV evaluations may not be the best for diagnosis of pancreatic fibrosis. Although our threshold-based approach helped minimize the impact of fatty infiltration, complete elimination of partial volume effects was not possible at this slice thickness. However, as this limitation was consistent across all subjects and our analysis focused on comparative differences between patients, we believe the impact on our primary findings was limited. Fifth, the timing of the equilibrium phase in our study may not have provided enough time for the contrast agent to equilibrate fully. However, Yoon et al. [26] demonstrated that an equilibrium phase of 180 s after contrast injection, as used in this study, provided a good balance between clinical and technical characteristics. Sixth, histological evaluation of fibrosis was not performed on surgical specimens because many patients received neoadjuvant therapy between the initial CT imaging and surgery. This treatment-induced fibrosis would have altered the tissue characteristics from their state at the time of fECV measurement. Finally, although we applied a thresholding process to the CT images to decrease the potential influence of pancreatic steatosis on fECV measurements, other factors, such as diabetes, were not included in the analysis and may have affected the results. In addition, future studies with larger cohorts must be carried out to investigate potential interactions between fECV values and chemotherapy efficacy, as pancreatic fibrosis may influence drug delivery and treatment response. Such analyses can contribute to developing individualized treatment strategies based on baseline pancreatic parenchymal characteristics.

In conclusion, our study demonstrated the significant prognostic value of fECV in the pancreatic parenchyma of noncancerous areas for OS in patients with PDAC. Further research is warranted to validate these findings in larger cohorts and assess the influence of additional factors on the prognostic value of fECV in PDAC.

Declaration of generative AI in scientific writing

We did not use any AI technology in the preparation of this manuscript.

Ethical approval and informed consent.

This study was approved by the Institutional Review Board at Osaka University Hospital (Approval Number: [20351]), and informed consent was waived in accordance with ethical regulations for retrospective studies, adhering to human rights declarations.

CRediT authorship contribution statement

Hideyuki Fukui: Conceptualization, Data curation, Formal analysis, Investigation, Methodology, Project administration, Resources, Software, Visualization, Writing – original draft. Yasunari Fukuda: Conceptualization, Methodology, Writing – review & editing. Hiromitsu Onishi: Data curation, Formal analysis, Investigation, Methodology, Project administration, Resources, Supervision, Validation, Writing – review & editing. Takashi Ota: Formal analysis, Investigation. Atsushi Nakamoto: Supervision. Toru Honda: Investigation. Ryo Aihara: Investigation. Yukihiro Enchi: Resources, Software. Daisaku Yamada: Resources. Shogo Kobayashi: Writing – review & editing. Hidetoshi Eguchi: Writing – review & editing. Mitsuaki Tatsumi: Writing – review & editing. Noriyuki Tomiyama: Writing – review & editing. All authors have read and approved the final version of the manuscript for publication.

Funding sources

The authors state that this work has not received any funding.

Data availability statements

The datasets used and/or analysed during the current study are available from the corresponding author on reasonable request.

CRediT authorship contribution statement

Hideyuki Fukui: Writing – original draft, Visualization, Software, Resources, Project administration, Methodology, Investigation, Formal analysis, Data curation, Conceptualization. **Yasunari Fukuda:** Writing – review & editing, Methodology, Conceptualization. **Hiromitsu Onishi:** Writing – review & editing, Validation, Supervision, Resources, Project administration, Methodology, Investigation, Formal analysis, Data curation. **Takashi Ota:** Investigation, Formal analysis. **Atsushi Nakamoto:** Supervision. **Toru Honda:** Investigation. **Ryo Aihara:** Investigation. **Yukihiro Enchi:** Software, Resources. **Daisaku Yamada:** Resources. **Shogo Kobayashi:** Writing – review & editing. **Hidetoshi Eguchi:** Writing – review & editing. **Mitsuaki Tatsumi:** Writing – review & editing. **Noriyuki Tomiyama:** Writing – review & editing.

Declaration of competing interest

The authors declare that they have no known competing financial interests or personal relationships that could have appeared to influence the work reported in this paper.

Acknowledgement

The authors thank Enago (www.enago.jp) for the English language review.

References

[1] K.Y. Elbanna, H.-J. Jang, T.K. Kim, Imaging diagnosis and staging of pancreatic ductal adenocarcinoma: a comprehensive review, Insights Imaging. 11 (2020) 58, https://doi.org/10.1186/s13244-020-00861-y.

[2] J.C. Chang, M. Kundranda, Novel diagnostic and predictive biomarkers in pancreatic adenocarcinoma, Int. J. Mol. Sci. 18 (2017) 667, https://doi.org/10.3390/ijms18030667.

[3] D. Xu, K. Zhang, M. Li, J.P. Neoptolemos, J. Wu, W. Gao, P. Wu, B. Cai, J. Yin, G. Shi, Z. Lu, K. Jiang, Y. Miao, Prognostic nomogram for resected pancreatic adenocarcinoma: a tripod-compliant retrospective long-term survival analysis, World J. Surg. 44 (2020) 1260–1269, https://doi.org/10.1007/s00268-019-05325-z.

[4] F. Wang, Y. Zhao, J. Xu, S. Shao, D. Yu, Development and external validation of a radiomics combined with clinical nomogram for preoperative prediction prognosis of resectable pancreatic ductal adenocarcinoma patients, Front. Oncol. 12 (2022) 1037672, https://doi.org/10.3389/fonc.2022.1037672.

[5] C. Cen, L. Liu, X. Li, A. Wu, H. Liu, X. Wang, H. Wu, C. Wang, P. Han, S. Wang, Pancreatic ductal adenocarcinoma at CT: a combined nomogram model to preoperatively predict cancer stage and survival outcome, Front. Oncol. 11 (2021) 594510, https://doi.org/10.3389/fonc.2021.594510.

[6] J.-F. Gao, Y. Pan, X.-C. Lin, F.-C. Lu, D.-S. Qiu, J.-J. Liu, H.-G. Huang, Prognostic value of preoperative enhanced computed tomography as a quantitative imaging biomarker in pancreatic cancer, World J. Gastroenterol. 28 (2022) 2468–2481, https://doi.org/10.3748/wjg.v28.i22.2468.

[7] J. Yao, Y. Shi, K. Cao, L. Lu, J. Lu, Q. Song, G. Jin, J. Xiao, Y. Hou, L. Zhang, DeepPrognosis: Preoperative prediction of pancreatic cancer survival and surgical margin via comprehensive understanding of dynamic contrast-enhanced CT imaging and tumor-vascular contact parsing, Med. Image Anal. 73 (2021) 102150, https://doi.org/10.1016/j.media.2021.102150.

[8] D.W. Shin, J. Park, J.-C. Lee, J. Kim, Y.H. Kim, J.-H. Hwang, Multi-phase, contrast-enhanced computed tomography-based radiomic prognostic marker of non-metastatic pancreatic ductal adenocarcinoma, Cancers 14 (2022) 2476, https://doi.org/10.3390/cancers14102476.

[9] H. Ni, G. Zhou, X. Chen, J. Ren, M. Yang, Y. Zhang, Q. Zhang, L. Zhang, C. Mao, X. Li, Predicting recurrence in pancreatic ductal adenocarcinoma after radical surgery using an ax-unet pancreas segmentation model and dynamic nomogram, Bioengineering 10 (2023) 828, https://doi.org/10.3390/bioengineering10070828.

[10] C. Palmquist, C. Dehlendorff, D. Calatayud, C.P. Hansen, J.P. Hasselby, J. S. Johansen, Prediction of unresectability and prognosis in patients undergoing

surgery on suspicion of pancreatic cancer using carbohydrate antigen 19-9, interleukin 6, and YKL-40, Pancreas 49 (2020) 53–61, https://doi.org/10.1097/mpa.0000000000001466.
[11] X. Cai, F. Gao, Y. Qi, G. Lan, X. Zhang, R. Ji, Y. Xu, C. Liu, Y. Shi, Pancreatic adenocarcinoma: quantitative CT features are correlated with fibrous stromal fraction and help predict outcome after resection, Eur. Radiol. 30 (2020) 5158–5169, https://doi.org/10.1007/s00330-020-06853-2.
[12] M.A. Attiyeh, J. Chakraborty, A. Doussot, L. Langdon-Embry, S. Mainarich, M. Gönen, V.P. Balachandran, M.I. D'Angelica, R.P. DeMatteo, W.R. Jarnagin, T. P. Kingham, P.J. Allen, A.L. Simpson, R.K. Do, Survival prediction in pancreatic ductal adenocarcinoma by quantitative computed tomography image analysis, Ann. Surg. Oncol. 25 (2018) 1034–1042, https://doi.org/10.1245/s10434-017-6323-3.
[13] N. Sengul Samanci, E. Çelik, O. Bagcilar, O. Tutar, C. Samanci, M. Velidedeoglu, A. E. Yassa, N.S. Demirci, F.H. Demirelli, Use of volumetric CT scanning to predict tumor staging and survival in pancreatic cancer patients that are to be administered curative resection, J. Surg. Oncol. 123 (2021) 1757–1763, https://doi.org/10.1002/jso.26455.
[14] Y. Fukukura, Y. Kumagae, R. Higashi, H. Hakamada, M. Nakajo, K. Maemura, S. Arima, T. Yoshiura, Extracellular volume fraction determined by equilibrium contrast-enhanced dual-energy CT as a prognostic factor in patients with stage IV pancreatic ductal adenocarcinoma, Eur. Radiol. 30 (2020) 1679–1689, https://doi.org/10.1007/s00330-019-06517-w.
[15] Y. Fukukura, Y. Kumagae, R. Higashi, H. Hakamada, K. Takumi, K. Maemura, M. Higashi, K. Kamimura, M. Nakajo, T. Yoshiura, Extracellular volume fraction determined by equilibrium contrast-enhanced multidetector computed tomography as a prognostic factor in unresectable pancreatic adenocarcinoma treated with chemotherapy, Eur. Radiol. 29 (2019) 353–361, https://doi.org/10.1007/s00330-018-5570-4.
[16] G. Noid, G. Godfrey, W. Hall, J. Shah, E. Paulson, P. Knechtges, B. Erickson, X. Allen Li, Predicting treatment response from extracellular volume fraction for chemoradiation therapy of pancreatic cancer, Int. J. Radiat. Oncol. Boil. Phys. 115 (2023) 803–808, https://doi.org/10.1016/j.ijrobp.2022.09.084.
[17] Z.J. Wang, T.T. Zhang, C. An, A.H. Ko, M. Tempero, E. Collisson, B.M. Yeh, Estimation of fractional extracellular space at CT for predicting chemotherapy response and survival in pancreatic ductal adenocarcinoma, Am. J. Roentgenol. 215 (2020) 610–616, https://doi.org/10.2214/ajr.19.22462.
[18] L. Zhu, X. Shi, H. Xue, H. Wu, G. Chen, H. Sun, Y. He, Z. Jin, Z. Liang, Z. Zhang, CT Imaging biomarkers predict clinical outcomes after pancreatic cancer surgery, Medicine 95 (2016) e2664.
[19] Y. Fukukura, Y. Kumagae, R. Higashi, H. Hakamada, M. Nakajo, K. Maemura, S. Arima, T. Yoshiura, Estimation of extracellular volume fraction with routine multiphasic pancreatic computed tomography to predict the survival of patients with stage IV pancreatic ductal adenocarcinoma, Pancreas 48 (2019) 1360–1366, https://doi.org/10.1097/mpa.0000000000001427.
[20] T. Sakuratani, S. Osada, J.Y. Tajima, K. Tanaka, S. Matsui, H. Imai, Y. Sasaki, H. Tomita, Y. Tanaka, N. Matsuhashi, K. Yoshida, Significance of histopathological evaluation of pancreatic fibrosis to predict postoperative course after pancreatic surgery, Anticancer Res 35 (2015) 1749–1756, https://doi.org/10.1016/j.pan.2016.06.380.
[21] K. Sofue, E. Ueshima, A. Masuda, S. Shirakawa, Y. Zen, Y. Ueno, Y. Tsujita, T. Yamaguchi, S. Yabe, T. Tanaka, N. Inomata, H. Toyama, T. Fukumoto, Y. Kodama, T. Murakami, Estimation of pancreatic fibrosis and prediction of postoperative pancreatic fistula using extracellular volume fraction in multiphasic contrast-enhanced CT, Eur. Radiol. 32 (2022) 1770–1780, https://doi.org/10.1007/s00330-021-08255-4.
[22] H. Fukui, H. Onishi, A. Nakamoto, T. Tsuboyama, T. Ota, K. Yano, Y. Enchi, D. Yamada, Y. Takeda, S. Kobayashi, Y. Fukuda, H. Eguchi, T. Matsui, M. Tatsumi, N. Tomiyama, Pancreatic fibrosis by extracellular volume fraction using contrast-enhanced computed tomography and relationship with pancreatic cancer, Eur. J. Radiol. 156 (2022) 110522, https://doi.org/10.1016/j.ejrad.2022.110522.
[23] D. Thomas, P. Radhakrishnan, Tumor-stromal crosstalk in pancreatic cancer and tissue fibrosis, Mol. Cancer 18 (2019) 14, https://doi.org/10.1186/s12943-018-0927-5.
[24] M. Erkan, S. Hausmann, C.W. Michalski, A.M. Schlitter, A.A. Fingerle, M. Dobritz, H. Friess, J. Kleeff, How fibrosis influences imaging and surgical decisions in pancreatic cancer, Front. Physio. 3 (2012) 389, https://doi.org/10.3389/fphys.2012.00389.
[25] M.V. Apte, J.S. Wilson, Mechanisms of pancreatic fibrosis, Dig. Dis. 22 (2004) 273–279, https://doi.org/10.1159/000082799.
[26] G. Klöppel, S. Detlefsen, B. Feyerabend, Fibrosis of the pancreas: the initial tissue damage and the resulting pattern, Virchows Arch. 445 (2004) 1–8, https://doi.org/10.1007/s00428-004-1021-5.
[27] P. Chen, Y. Wang, X. Fang, X. Wang, G. Wang, Prognostic significance of peritumoral fibrosis after resection of pancreatic head cancer, Oncol. Lett. 19 (2020) 1235–1240, https://doi.org/10.3892/ol.2019.11181.
[28] G. Digiacomo, F. Volta, I. Garajova, R. Balsano, A. Cavazzoni, Biological hallmarks and new therapeutic approaches for the treatment of PDAC, Life 11 (2021) 843, https://doi.org/10.3390/life11080843.
[29] Working Group IAP/APA Acute Pancreatitis Guidelines, IAP/APA evidence-based guidelines for the management of acute pancreatitis, Pancreatology 13 (2013) e1–e15, https://doi.org/10.1016/j.pan.2013.07.063.
[30] Y. Shinagawa, K. Sakamoto, K. Sato, E. Ito, H. Urakawa, K. Yoshimitsu, Usefulness of new subtraction algorithm in estimating degree of liver fibrosis by calculating extracellular volume fraction obtained from routine liver CT protocol equilibrium phase data: Preliminary experience, Eur. J. Radiol. 103 (2018) 99–104, https://doi.org/10.1016/j.ejrad.2018.04.012.
[31] H. Fukui, H. Onishi, A. Nakamoto, T. Tsuboyama, T. Ota, T. Honda, K. Kiso, E. Yoshidome, Y. Enchi, M. Tatsumi, N. Tomiyama, Hepatic and pancreatic extracellular volume fraction analysis using contrast-enhanced CT in patients with diabetes mellitus and pre-diabetes, Jpn. J. Radiol. 42 (2024) 599–611, https://doi.org/10.1007/s11604-024-01531-5.
[32] J.H. Yoon, J.M. Lee, E. Klotz, J.H. Jeon, K.-B. Lee, J.K. Han, B.I. Choi, Estimation of hepatic extracellular volume fraction using multiphasic liver computed tomography for hepatic fibrosis grading, Invest. Radiol. 50 (2015) 290–296, https://doi.org/10.1097/rli.0000000000000123.
[33] M.H. Zissen, Z.J. Wang, J. Yee, R. Aslam, A. Monto, B.M. Yeh, Contrast-enhanced CT quantification of the hepatic fractional extracellular space: correlation with diffuse liver disease severity, Am. J. Roentgenol. 201 (2013) 1204–1210, https://doi.org/10.2214/ajr.12.10039.
[34] M.-Y. Su, Y.-S. Huang, E. Niisato, K. Chow, J.-M.-J. Juang, C.-K. Wu, H.-Y. Yu, L.-Y. Lin, S.-C. Yang, Y.-C. Chang, Is a timely assessment of the hematocrit necessary for cardiovascular magnetic resonance–derived extracellular volume measurements? J. Cardiovasc. Magn. Reson. 22 (2020) 77, https://doi.org/10.1186/s12968-020-00689-x.

Glossary

Extracellular volume fraction (fECV):: A quantitative imaging parameter derived from contrast-enhanced computed tomography that reflects the proportion of tissue volume that is extracellular space, influenced by factors such as vascularity, cellularity, and fibrosis.
Pancreatic ductal adenocarcinoma (PDAC):: The most common type of pancreatic cancer that originates in the cells lining the ducts that carry pancreatic digestive enzymes.
Recurrence-free survival (RFS):: The length of time after primary treatment for a cancer ends that the patient survives without any signs or symptoms of that cancer.
Overall survival (OS):: The length of time from either the date of diagnosis or the start of treatment for a disease that patients diagnosed with the disease are still alive.
Contrast-enhanced computed tomography (CE-CT):: An imaging technique that uses X-rays to create detailed images of the inside of the body after administration of a contrast agent.
TNM staging:: A classification system used to describe the stage of a cancer based on the size and extent of the primary tumor (T), involvement of regional lymph nodes (N), and the presence or absence of distant metastases (M).
Neoadjuvant therapy:: Treatment given as a first step to shrink a tumor before the main treatment, usually surgery, is given.
Adjuvant therapy:: Additional treatment given after the primary treatment to lower the risk of cancer recurrence.